Pergamon

0277–5387(95)00059–3

Polyhedron Vol. 14, No. 17–18, pp. 2491–2497, 1995
Copyright © 1995 Elsevier Science Ltd
Printed in Great Britain. All rights reserved
0277–5387/95 $9.50+0.00

STRUCTURAL INVESTIGATION OF TIN(IV) ALKOXIDE COMPOUNDS—II. SOLID STATE AND SOLUTION STRUCTURAL CHARACTERIZATION OF $[Sn(O\text{-}i\text{-}Bu)_4 \cdot HO\text{-}i\text{-}Bu]_2$

CLIVE D. CHANDLER, JAMES CARUSO and MARK J. HAMPDEN-SMITH*

Department of Chemistry and Center for Micro-Engineered Ceramics, University of New Mexico, Albuquerque, NM 87131, U.S.A.

and

ARNOLD L. RHEINGOLD

Department of Chemistry, University of Delaware, Newark, DE 19716, U.S.A.

(*Received* 31 *October* 1994; *accepted* 11 *January* 1995)

Abstract—The trans-alcoholysis reaction between $Sn(O\text{-}t\text{-}Bu)_4$ and an excess of HO-i-Bu results in quantitative formation of $[Sn(O\text{-}i\text{-}Bu)_4 \cdot HO\text{-}i\text{-}Bu]_2$. This compound was structurally characterized in solution by ^1H, ^{13}C and ^{119}Sn NMR spectroscopy and in the solid-state by single-crystal X-ray diffraction. The molecular structure consists of an edge-shared bi-octahedral Sn_2 unit with an intramolecular hydrogen bridge between the coordinated alcohol and metal alkoxide. The dynamic behaviour of this compound was studied in solution and revealed the presence of an intramolecular proton exchange process that was fast on the NMR time-scale.

The sol–gel chemistry of metal alkoxide compounds is currently a topic of great scientific and technological interest.[1–5] Silicon alkoxide compounds have received the greatest attention because the steps of hydrolysis and condensation can be separated and so significant control over the evolution of microstructure during formation of SiO_2 can be achieved.[3] Silicon alkoxide compounds undergo slow and reversible hydrolysis and condensation reactions, they are monomeric and four-coordinate and show no tendency to oligomerize. In contrast, other metal alkoxide compounds can exhibit a variety of coordination geometries and coordination numbers ranging from 2 to 8, and they readily oligomerize in the absence of other donor molecules to satisfy their coordination number.[5–9] The rates of hydrolysis and condensation appear to be fast and irreversible, although little quantitative data are available. As a result, the factors that control the evolution of microstructure in non-silicate metal oxide systems are significantly more complex and poorly understood compared to the silicate system. Some insight into this problem is being obtained by studies of the hydrolysis of $Ti(OR)_4$ compounds, where a variety of titanium oxo-alkoxide complexes have been isolated and identified.[10,11]

When considering strategies to control structural evolution during the conversion of a metal alkoxide to a metal oxide by hydrolytic routes, it is important to understand the solution structure and dynamic behaviour of the metal alkoxide starting materials. If the starting materials rearrange on the same time-scale that hydrolysis reactions occur, structural dimensionality imposed by a particular metal alkoxide or modified metal alkoxide precursor geometry may be lost.[12,13] To investigate these possi-

---

* Author to whom correspondence should be addressed.

bilities, we have been studying the chemistry of tin(IV) alkoxide compounds[14–18] as a model system, since these species display a chemistry prototypical of non-silicate metal alkoxide compounds and can be characterized in solution with the aid of NMR spectroscopy via ^{119}Sn and ^{117}Sn NMR active isotopes.[19] It has been demonstrated that the magnitude of the two-bond ^{119}Sn–^{13}C coupling constant is a sensitive spectroscopic probe to allow distinction between terminal and doubly bridging alkoxide ligands in solution.[15] Using this criterion, it has been shown that $[\mathrm{Sn(O\text{-}i\text{-}Pr)_4 \cdot HO\text{-}i\text{-}Pr}]_2$ is dimeric in solution and undergoes a dynamic rearrangement involving intramolecular proton transfer below 0°C and reversible dissociation of the coordinated alcohol ligand at and above room temperature. Hydrogen bonding in these systems is likely to be an important structural feature, since hydrolysis and condensation reactions are often carried out in the presence of alcohol solvents.[20]

Here we report the solid-state single crystal X-ray diffraction structure and solution structural characterization of $[\mathrm{Sn(O\text{-}i\text{-}Bu)_4 \cdot HO\text{-}i\text{-}Bu}]_2$. This alkoxide ligand was chosen for comparison to the structural data already obtained for other homoleptic tin(IV) alkoxide compounds with tertiary (—O-t-Bu)[15] and secondary (—O-i-Pr)[15] alkoxide ligands.

EXPERIMENTAL

General procedures

All manipulations were carried out under dry (molecular sieves) dinitrogen using standard Schlenk techniques.[21] All hydrocarbon and ethereal solvents were dried and distilled from sodium benzophenone ketyl and stored over 4 Å molecular sieves. The reagents were purchased from Aldrich Chemical Co. and used without further purification. Elemental analyses were performed either by Oneida Research Services, New York, or by Ms R. Ju at the University of New Mexico, Department of Chemistry. NMR data were recorded on a Bruker AC-250P NMR spectrometer by using the protio impurities of the deuterated solvents as references for the ^{1}H NMR and the ^{13}C resonance of the solvents as reference for ^{13}C{^{1}H} NMR spectroscopy. Temperatures were calibrated with either ethyleneglycol or methanol. ^{119}Sn NMR data were recorded on the same instrument using tetraethyltin as an external reference. IR data were recorded on a Perkin–Elmer Model 1620 FTIR spectrophotometer. Mass spectra were recorded on a Finnegan GC-mass spectrometer.

Syntheses

Preparation of $[\mathrm{Sn(O\text{-}i\text{-}Bu)_4 \cdot HO\text{-}i\text{-}Bu}]_2$. $\mathrm{Sn(O\text{-}t\text{-}Bu)_4}$ (5.3 g) was dissolved in 10 cm^3 of HO-i-Bu and stirred for 15 min, during which time a white precipitate formed. The solvent was removed under high vacuum, leaving a white solid. The solid was dissolved in a 1 : 1 mixture of pentane and HO-i-Bu, stirred for 10 min, then the volatile components were removed *in vacuo* and a further aliquot of pentane–HO-i-Bu was added, stirred and pumped dry. The yield of $[\mathrm{Sn(O\text{-}i\text{-}Bu)_4 \cdot HO\text{-}i\text{-}Bu}]_2$ was quantitative.

Spectroscopic data. ^{1}H NMR data (ppm; 250 MHz, 273 K, C_6D_6): 4.1 [d, 7 Hz, 4H, $^2J_{\mathrm{H\text{-}Sn}} = 38$ Hz, $\mathrm{OC}\mathit{H}_2\mathrm{CH(CH_3)_2}$]; 3.93 [d, 7 Hz, 4H, $^2J_{\mathrm{H\text{-}Sn}} = 25$ Hz, $\mathrm{OC}\mathit{H}_2\mathrm{CH(CH_3)_2}$]; 3.89 [d, 7 Hz, 4H, $^2J_{\mathrm{H\text{-}Sn}} = 30$ Hz, $\mathrm{OC}\mathit{H}_2\mathrm{CH(CH_3)_2}$]; 2.64 [septet, 1H, $\mathrm{HOCH_2C}\mathit{H}\mathrm{(CH_3)_2}$]; 2.10 [septet, 2H, $\mathrm{HOCH_2C}\mathit{H}\mathrm{(CH_3)_2}$]; 1.96 [septet, 2H, $\mathrm{OCH_2C}\mathit{H}\mathrm{(CH_3)_2}$]; 1.25 [d, 6 Hz, 6H, $\mathrm{HOCH_2CH(C}\mathit{H}_3)_2$]; 1.10 [d, 6 Hz, 12H, $\mathrm{HOCH_2CH(C}\mathit{H}_3)_2$]; 1.00 [d, 6 Hz, 12H, $\mathrm{HOCH_2CH(C}\mathit{H}_3)_2$].

^{13}C{^{1}H} NMR data (ppm; 62.9 MHz, 273 K, C_6D_6): 72.90 [s, $^2J_{^{13}\mathrm{C\text{-}Sn}} = 19.5$ Hz (30%), $\mathrm{O}\mathit{C}\mathrm{H_2CH(CH_3)_2}$]; 72.74 [s, $^2J_{^{13}\mathrm{C\text{-}Sn}} = 41$ Hz (18%), $\mathrm{O}\mathit{C}\mathrm{H_2CH(CH_3)_2}$]; 72.08 [s, $^2J_{^{13}\mathrm{C\text{-}Sn}} = 19.4$ Hz (21%), $\mathrm{O}\mathit{C}\mathrm{H_2CH(CH_3)_2}$]; 32.91 [s, $^3J_{^{13}\mathrm{C\text{-}Sn}} = 59$ Hz, $\mathrm{OCH_2}\mathit{C}\mathrm{H(CH_3)_2}$]; 31.43 [s, $^3J_{^{13}\mathrm{C\text{-}Sn}} = 11.3$ Hz, $\mathrm{OCH_2}\mathit{C}\mathrm{H(CH_3)_2}$]; 30.50 [s, $^3J_{^{13}\mathrm{C\text{-}Sn}} = 5$ Hz, $\mathrm{OCH_2}\mathit{C}\mathrm{H(CH_3)_2}$]; 19.69 [s, $\mathrm{OCH_2CH(}\mathit{C}\mathrm{H_3)_2}$]; 19.46 [s, $\mathrm{OCH_2CH(}\mathit{C}\mathrm{H_3)_2}$]; 19.37 [s, $\mathrm{OCH_2CH(}\mathit{C}\mathrm{H_3)_2}$].

^{119}Sn{^{1}H} NMR data (93.2 MHz, 30°C, C_7D_8): -634.4 ppm. $^2J_{^{119}\mathrm{Sn}\text{-}^{117}\mathrm{Sn}} = 300$ Hz (8%).

Single crystal X-ray diffraction data

A colourless crystal obtained by crystallization from toluene at -30°C was mounted in a capillary under a nitrogen atmosphere. The unit cell parameters were determined from a least squares fit of 25 reflections ($20° < 2\theta < 25°$). Preliminary photographic characterization showed $\bar{1}$ Laue symmetry. *E*-statistics suggested the centrosymmetric alternative and the chemically sensible results of refinement proved the choice of $P\bar{1}$ to be correct. No correction for absorption was applied (low *m*, well-shaped crystal, $T_{\max}/T_{\min} = 1.122$).

The structure was solved by Patterson solution, which located the tin atom. The remaining non-hydrogen atoms were located through subsequent Fourier syntheses. All non-hydrogen atoms were refined with anisotropic thermal parameters. Each of the isobutyl groups was disordered. Carbon atoms C(1), C(5), C(9), C(13) and C(17) were all disordered over two sites and were modelled as 1 : 1

Table 1. Crystallographic data for $[Sn(O\text{-}i\text{-}Bu)_4 \cdot (HO\text{-}i\text{-}Bu)]_2$

Formula	$(C_{20}H_{45}O_5Sn)_2$	V (Å^3)	1363.7(8)
Formula weight	968.53	Z	1
Space group	$P\bar{1}$	D_{calc} (g cm^{-3})	1.179
a (Å)	19.544(4)	μ(Mo-K_α) (cm^{-1})	9.59
b (Å)	11.939(4)	Temp. (K)	297
c (Å)	12.615(4)	T_{max}/T_{min}	1.122
α (°)	111.091(27)	Radiation	Mo-K_α ($\lambda = 0.71073$ Å)
β (°)	96.652(28)	$R(F)$ (%)	7.61
χ (°)	107.854(28)	$R(wF)$ (%)	8.11

contributions. Hydrogen atom contributions were ignored. The crystal, data collection and refinement parameters are collected in Table 1. Table 2 contains relevant bond distances and angles. All computer programs and sources of the scattering factors are contained in the SHELXTL program library (5.1) [G. Sheldrick; Nicolet (Siemens), Madison, WI]. A complete listing of crystallographic data, bond lengths and angles and observed and calculated structure factors are available as supplementary materials and have been deposited with the Cambridge Crystallographic Data Centre.

RESULTS AND DISCUSSION

The isobutanol adduct of tin(IV) isobutoxide was prepared by the alcoholysis of $Sn(O\text{-}t\text{-}Bu)_4$ using an excess of HO-i-Bu, a standard procedure for the replacement of a more sterically demanding alkoxide with a less sterically demanding one.[5] The crystalline product was isolated by crystallization from toluene at -30°C. The ^{1}H and ^{13}C{^{1}H} NMR data for the product were consistent with the empirical formula $[Sn(O\text{-}i\text{-}Bu)_4 \cdot HO\text{-}i\text{-}Bu]_n$ and the ^{119}Sn{^{1}H} NMR spectrum exhibited a $^2J_{^{119}Sn-^{117}Sn}$ consistent with the presence of a dimeric unit. These data are qualitatively analogous to the corresponding NMR data for $[Sn(O\text{-}i\text{-}Pr)_4 \cdot HO\text{-}i\text{-}Pr]_2$, although the exchange behaviour appears different. In order to compare the structure and solution behaviour of $[Sn(O\text{-}i\text{-}Bu)_4 \cdot HO\text{-}i\text{-}Bu]_2$ with $[Sn(O\text{-}i\text{-}Pr)_4 \cdot HO\text{-}i\text{-}Pr]_2$, the structure and solution dynamic behaviour of $[Sn(O\text{-}i\text{-}Pr)_4 \cdot HO\text{-}i\text{-}Pr]_2$[15] will be reviewed briefly, followed by a discussion of the structure and solution dynamic behaviour of $[Sn(O\text{-}i\text{-}Bu)_4 \cdot HO\text{-}i\text{-}Bu]_2$.

In the solid state, $[Sn(O\text{-}i\text{-}Pr)_4 \cdot HO\text{-}i\text{-}Pr]_2$ exhibits the structure **1** shown in Fig. 1.[15] The most noteworthy feature relevant to this discussion is the presence of an asymmetric intramolecular hydrogen bond which was evident in the difference between the Sn—O bond lengths of the hydrogen-bonded alkoxide compared to the coordinated alcohol. Solution ^{1}H and ^{13}C{^{1}H} NMR spectra consistent with this structure were observed at low temperature (< -60°C), which on warming underwent a series of changes consistent with the interpretation given in Fig. 1, where intramolecular proton transfer occurred between the original coordinated alcohol and adjacent alkoxide and, finally, at room temperature, a single time-averaged type of O-i-Pr group was observed, consistent with dis-

Table 2. Relevant bond lengths (Å) and angles (°) for $[Sn(O\text{-}i\text{-}Bu)_4 \cdot HO\text{-}i\text{-}Bu]_2$

Sn—O(1)	2.094(5)	Sn—O(2)	2.108(9)
Sn—O(3)	1.932(7)	Sn—O(4)	2.114(8)
Sn—O(5)	1.943(9)	Sn—O(1A)	2.069(7)
Sn···Sn(A)	3.336(1)		
O(1)—Sn—O(2)	81.6(3)	O(1)—Sn—O(3)	165.0(3)
O(2)—Sn—O(3)	95.1(3)	O(1)—Sn—O(4)	81.8(3)
O(2)—Sn—O(4)	159.5(2)	O(3)—Sn—O(4)	97.9(3)
O(1)—Sn—O(5)	93.4(3)	O(2)—Sn—O(5)	96.3(4)
O(3)—Sn—O(5)	101.5(3)	O(4)—Sn—O(5)	96.5(3)
O(1)—Sn—O(1A)	73.5(3)	O(2)—Sn—O(1A)	81.9(3)
O(3)—Sn—O(1A)	91.6(3)	O(4)—Sn—O(1A)	82.0(3)
O(5)—Sn—O(1A)	166.9(2)	Sn—O(1)—Sn(A)	106.5(3)

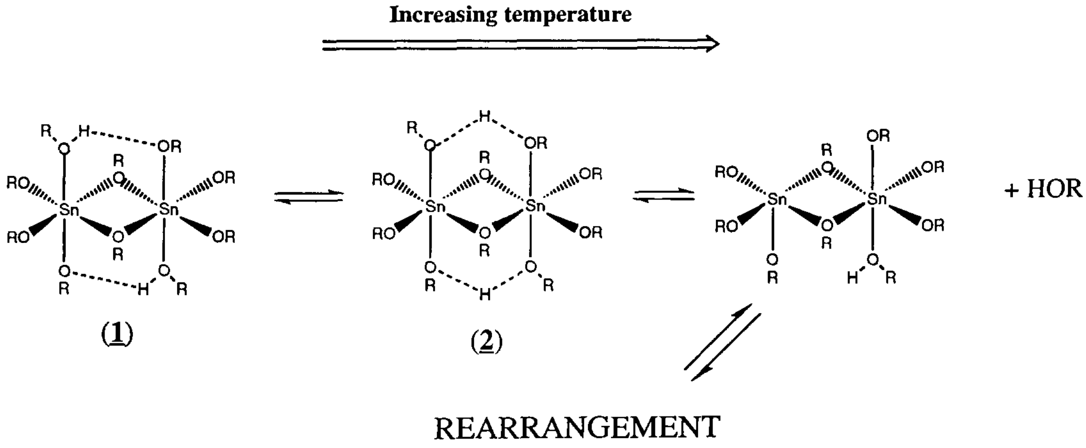

Fig. 1. Schematic representation of the dynamic solution behaviour of $[Sn(O\text{-}i\text{-}Pr)_4 \cdot HO\text{-}i\text{-}Pr]_2$.

sociation of the coordinated alcohol and alcohol–alkoxide exchange. The ^1H NMR resonance of added HO-i-Pr also exchanged with the single O-i-Pr resonance of $[Sn(O\text{-}i\text{-}Pr)_4 \cdot HO\text{-}i\text{-}Pr]_2$ at room temperature, but at lower temperatures no added HO-i-Pr/O-i-Pr exchange was observed, consistent with the interpretation above.

In the case of $[Sn(O\text{-}i\text{-}Bu)_4 \cdot HO\text{-}i\text{-}Bu]_2$, the solid-state structural data derived from single-crystal X-ray diffraction confirmed the dimeric nature of this compound and an ORTEP plot is shown in Fig. 2. The relevant bond lengths and angles are presented in Table 2. Unfortunately, the quality of the crystallographic data is not as good as that obtained for $[Sn(O\text{-}i\text{-}Pr)_4 \cdot HO\text{-}i\text{-}Pr]_2$ and no conclusions are drawn based on the hydrocarbon portion of this molecule. This also prevents distinction between the presence of asymmetric and symmetric intramolecular hydrogen bridges. However, the distortion of Sn—O(2) and Sn—O(4) from octahedral geometry about tin(IV) is consistent with the presence of a hydrogen bridge. The Sn—O(3) and Sn—O(5) distances of 1.932(7) and 1.943(9) Å, respectively, are in the range expected for terminal alkoxide ligands {1.964(7) and 1.923(7) Å for $[Sn(O\text{-}i\text{-}Pr)_4 \cdot HO\text{-}i\text{-}Pr]_2$}. However, Sn—O(2) and Sn—O(4) have similar values that lie in the range expected for a bridging alkoxide ligand analogous to Sn—O(1) and Sn—O(1a) of approximately 2.10 Å. This is in contrast to the structure of $[Sn(O\text{-}i\text{-}Pr)_4 \cdot HO\text{-}i\text{-}Pr]_2$, where the Sn—O distances of the hydrogen-bonded O-i-Pr [2.098(6) Å] and coordinated HO-i-Pr [2.142(6) Å] could be distinguished. Thus, in the solid-state structure of

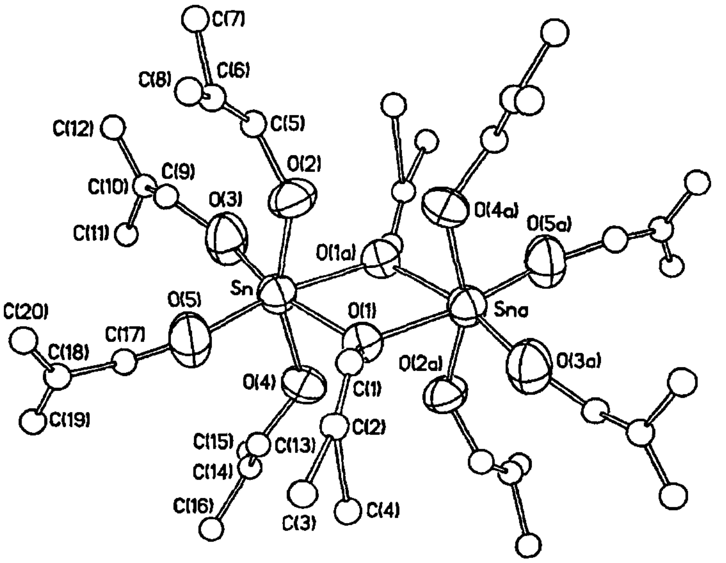

Fig. 2. Molecular structure of $[Sn(O\text{-}i\text{-}Bu)_4 \cdot HO\text{-}i\text{-}Bu]_2$ as determined by single-crystal X-ray diffraction.

[Sn(O-i-Bu)$_4$·HO-i-Bu]$_2$, the hydrogen bonding appears symmetric between Sn—O(2) and Sn—O(4a), although a superposition of asymmetrically bridged structures and a solid-state dynamic exchange process cannot be ruled out on the basis of these data.

The structural core of [Sn(OR)$_4$·HOR]$_2$ (R = i-Pr, i-Bu) is also found for a variety of other homoleptic tetravalent metal alkoxide compounds, including [M(O-i-Pr)$_4$·HO-i-Pr]$_2$, where M = Zr,[20] Hf[20] or Ce.[20] In the case of the zirconium and cerium analogues, the hydrogen bonding was also found to be markedly asymmetric in the solid-state structures. The presence of intramolecular hydrogen bonding as a general structural feature of metal–organic complexes has also been addressed in relation to metal–organic complexes in general, as well as metal alkoxide complexes in particular.[20]

The solution NMR data for [Sn(O-i-Bu)$_4$·HO-i-Bu]$_2$ also reveal a different situation to that observed in the case of [Sn(O-i-Pr)$_4$·HO-i-Pr]$_2$. At room temperature, the ^{1}H NMR spectrum (toluene-d_8) reveals the presence of the coordinated HO-i-Bu through the resonance for the OH proton at 10.06 ppm together with a set of slightly broadened resonances consistent with three types of O-i-Bu ligands in a 2:2:1 ratio. On cooling to 273 K, the resonances sharpen, but no further splitting or exchange is observed, even on cooling to lower temperatures (198 K). The ^{1}H NMR spectrum at 273 K is consistent with structure **2** in Fig. 1, where the two O-i-Bu ligands of relative intensity 2 can be assigned to the terminal and hydrogen-bonded ligands (O-i-Bu and HO-i-Bu in rapid exchange), and the bridging O-i-Bu ligands are unique. The OCH_2 and $CHMe_2$ groups are non-diastereotopic, consistent with this interpretation. Although not observed in the case of [Sn(O-i-Pr)$_4$·HO-i-Pr]$_2$, $^3J_{^{119,117}\mathrm{Sn{-}OCH_2}}$ is observed for [Sn(O-i-Bu)$_4$·HO-i-Bu]$_2$, with values of 38 Hz for the O-i-Bu group of relative intensity 1 and 30 Hz and 25 Hz for the two O-i-Bu groups with relative intensity 2.

In the ^{13}C{^{1}H} NMR spectrum, the peaks were sharpest at 273 K and no changes in the spectrum were observed on cooling to lower temperatures. In the OCH_2— region, three resonances were observed in the approximate ratio 2:2:1, each with ^{119,117}Sn satellites. Of the resonances of relative intensity 2, one has ^{119,117}Sn satellites with a coupling constant of 41 Hz and 18% natural abundance and the other has a 19 Hz coupling constant with 21% natural abundance. These values are consistent with a terminal alkoxide ligand and a bridging alkoxide ligand, respectively, with the bridging alkoxide ligand adjacent to only one tin centre (by integration). We assign the latter resonance to the hydrogen-bonded, exchanging O-i-Bu/HO-i-Bu pair, according to the criteria for assignment of $^2J_{^{119}\mathrm{SnO{-}^{13}C}}$ coupling constants. The O—^{13}C resonance of relative intensity 1 has a $^2J_{^{119,117}\mathrm{SnO{-}^{13}C}}$ of 20 Hz with 30% natural abundance. This is consistent with an O-i-Bu ligand bridging two tin centres. The methine carbons, also present in the ratio 2:2:1, exhibit $^3J_{^{119,117}\mathrm{SnOC{-}^{13}C}}$ couplings of 59 Hz (15%), 12 Hz (15%) and 6 Hz (30%), respectively, which we assign to the terminal O-i-Bu, bridging O-i-Bu/HO-i-Bu and doubly tin bridging O-i-Bu, respectively.

On heating to 363 K, the peaks in the ^{1}H NMR spectrum broadened significantly, but do not appear to reach a high temperature exchange limit. The methyl groups appear as a single doublet at their population-weighted average chemical shift, but the distinction between an exchange process and accidental degeneracy cannot be distinguished from these data.

Addition of three equivalents of HO-i-Bu results in exchange broadening of the ^{1}H NMR resonances between the HO-i-Bu peaks and all the [Sn(O-i-Bu)$_4$·HO-i-Bu]$_2$ peaks at high temperatures (363 K), but at 273 K, no exchange was observed between [Sn(O-i-Bu)$_4$·HO-i-Bu]$_2$ and the added alcohol.

We interpret these data as follows. The solution structure of [Sn(O-i-Bu)$_4$·HO-i-Bu]$_2$ at 273 K is as shown in Fig. 3, with a symmetrically bridging hydrogen from the coordinated alcohol making this pair of O-i-Bu and HO-i-Bu indistinguishable by ^{1}H and ^{13}C{^{1}H} NMR spectroscopy. The intramolecular proton transfer process is fast on the NMR time-scale at this temperature and has an activation barrier that is lower than that of [Sn(O-i-Pr)$_4$·HO-i-Pr]$_2$, which can be observed on the NMR time-scale ($\Delta G\ddagger < 11.9$ kcal mol^{-1}) given that the frequency separation of the exchanging peaks is approximately the same in both cases. The barrier to dissociation of the coordinated alcohol is probably higher for [Sn(O-i-Bu)$_4$·HO-i-Bu]$_2$ than [Sn(O-i-Pr)$_4$·HO-i-Pr]$_2$ as indicated by the high temperature ^{1}H NMR data and the exchange experiment with HO-i-Bu. It appears that [Sn(O-i-Bu)$_4$·HO-i-Bu]$_2$ retains its coordinated alcohol more tenaciously than [Sn(O-i-Pr)$_4$·HO-i-Pr]$_2$.

These results can be compared with the exchange behaviour of other metal alkoxide compounds with their parent alcohols. The species Sn(O-t-Bu)$_4$ does not coordinate HO-t-Bu in the ground state, but a series of experiments investigating the kinetics of exchange between Sn(O-t-Bu)$_4$ and HO-t-Bu reveal a transition state consistent with the formation of a five-coordinate associated intermediate [Sn(O-t-Bu)$_4$·HO-t-Bu], as shown in Fig. 4.[22]

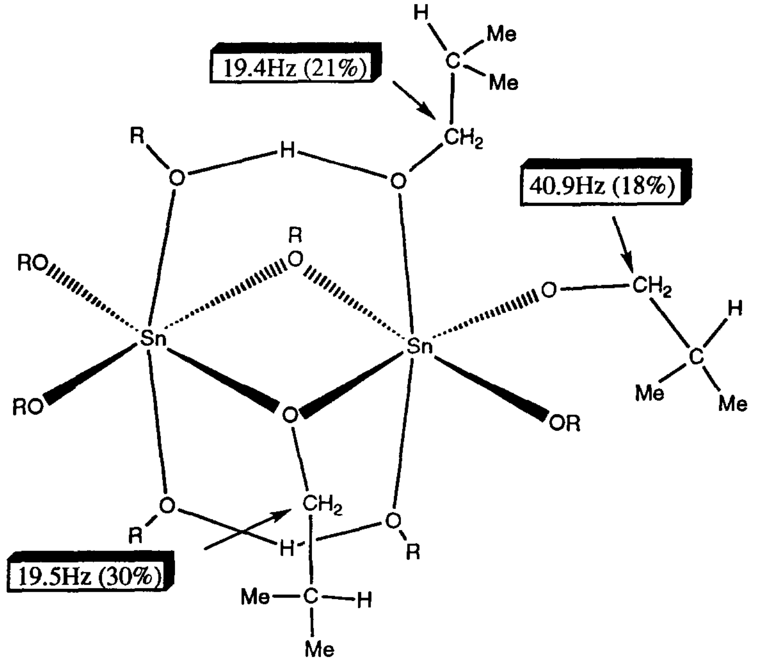

Fig. 3. Schematic representation of the solution structure of $[Sn(O\text{-}i\text{-}Bu)_4 \cdot HO\text{-}i\text{-}Bu]_2$ at 273 K.

The origin of these different exchange effects between homoleptic metal alkoxide compounds and their parent alcohols may lie in either the steric or electronic differences between these alcohols and alkoxide ligands. We favour the steric interpretation with the following argument. The availability of a vacant coordination site at the tin centre in a tin(IV) alkoxide compound is strongly influenced by the size of the alkoxide substituent. This is evidenced by the observation that $Sn(O\text{-}t\text{-}Bu)_4$ is monomeric, while $[Sn(O\text{-}i\text{-}Pr)_4 \cdot HO\text{-}i\text{-}Pr]_2$ and $[Sn(O\text{-}i\text{-}Bu)_4 \cdot HO\text{-}i\text{-}Bu]_2$ are dimeric and $[Sn(OEt)_4]_4$ is tetrameric. In order to complete the tin(IV) coordination sphere, $[Sn(O\text{-}i\text{-}Pr)_4 \cdot HO\text{-}i\text{-}Pr]_2$ and $[Sn(O\text{-}i\text{-}Bu)_4 \cdot HO\text{-}i\text{-}Bu]_2$ not only dimerize, but also coordinate one molecule of alcohol per tin centre. The "pocket" or coordination volume available to HO-i-Bu in $[Sn(O\text{-}i\text{-}Bu)_4 \cdot HO\text{-}i\text{-}Bu]_2$ is larger than that available to HO-i-Pr in $[Sn(O\text{-}i\text{-}Pr)_4 \cdot HO\text{-}i\text{-}Pr]_2$ due to the larger steric demands of —O-i-Pr ligands compared to —O-i-Bu ligands. In addition, HO-i-Pr itself is sterically more demanding than HO-i-Bu, which creates more repulsive steric interactions in $[Sn(O\text{-}i\text{-}Pr)_4 \cdot HO\text{-}i\text{-}Pr]_2$ compared to $[Sn(O\text{-}i\text{-}Bu)_4 \cdot HO\text{-}i\text{-}Bu]_2$.

Reactions involving metal alkoxide compounds, whether it be their synthesis or their use in reactions to form other materials such as metal oxides, are frequently carried out in the presence of a large excess of the parent alcohol. It is therefore likely that if the alcohol can coordinate to the metal centre, and if a large excess of alcohol is present, the alcohol may have a profound influence in the course of the reaction. As a result of this study and a comparison with analogous studies of the alcohol–alkoxide exchange rates in $[Sn(O\text{-}i\text{-}Pr)_4 \cdot HO\text{-}i\text{-}Pr]_2$ and $Sn(O\text{-}t\text{-}Bu)_4$ with added HO-t-Bu, we propose that the tin centre in $[Sn(O\text{-}i\text{-}Bu)_4 \cdot HO\text{-}i\text{-}Bu]_2$ is the least accessible to the parent alcohol molecule, or in other words is the least likely to yield its coordination site because its exchange rate with added alcohol is observed to be the slowest.

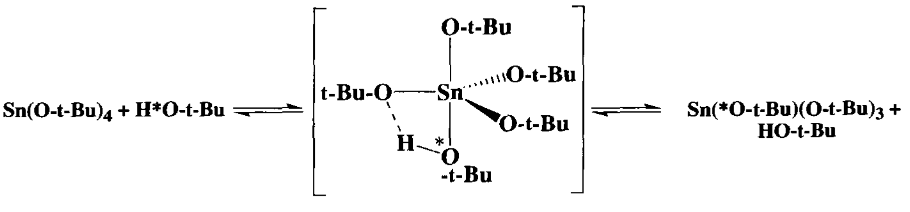

Fig. 4. Schematic representation of the solution dynamic behaviour of $Sn(O\text{-}t\text{-}Bu)_4$ in the presence of added HO-t-Bu.

These observations may have implications in the hydrolysis of metal alkoxide compounds in the hydrolytic sol–gel approach to prepare metal oxides.

Acknowledgements—We thank the Air Force Office of Scientific Research and the UNM/NSF Center for Micro-Engineered Ceramics for financial support of this work. We thank the NSF Chemical Instrumentation Program for the purchase of a low-field NMR instrument.

REFERENCES

1. C. J. Brinker and G. W. Scherer, *Sol–Gel Science: The Physics and Chemistry of Sol–Gel Processing.* Academic Press, Boston (1990).
2. R. J. Brooke (Ed.), *Concise Encyclopedia of Advanced Ceramic Material.* Pergamon Press, Oxford (1991).
3. L. C. Klein, *Sol–Gel Technology for Thin Films, Fibers, Preforms, Electronics and Specialty Shapes.* Noyes, Park Ridge (1988).
4. D. C. Bradley, *Chem Rev.* 1989, **89**, 1317.
5. D. C. Bradley, R. C. Mehrotra and D. P. Gaur, *Metal Alkoxides.* Academic Press, London (1978).
6. J. Livage, M. Henry and C. Sanchez, *Prog. Solid State Chem.* 1989, **18**, 259.
7. C. D. Chandler, C. Roger and M. J. Hampden-Smith, *Chem. Rev.* 1993, **93**, 1205.
8. L. G. Hubert-Pfalzgraf, *New J. Chem.* 1987, **11**, 663.
9. K. G. Caulton and L. G. Hubert-Pfalzgraf, *Chem. Rev.* 1990, **90**, 969.
10. V. W. Day, T. A. Eberspacher, W. G. Klemperer, C. W. Park and F. S. Rosenberg, *J. Am. Chem. Soc.* 1991, **113**, 8190.
11. V. W. Day, T. A. Eberspacher, W. G. Klemperer and C. W. Park, *J. Am. Chem. Soc.* 1993, **115**, 8469.
12. J. Livage, M. Henry, J. P. Jolivet and C. Sanchez, *MRS Bull.* 1990, **18**.
13. J. Livage, M. Henry, J. P. Jolivet and C. Sanchez, *J. Mater. Educ.* 1991, **13**, 233.
14. M. J. Hampden-Smith, D. E. Smith and E. N. Duesler, *Inorg. Chem.* 1989, **28**, 3399.
15. M. J. Hampden-Smith, T. A. Wark, A. L. Rheingold and J. C. Huffman, *Can. J. Chem.* 1990, **69**, 121.
16. M. J. Hampden-Smith, T. A. Wark and C. J. Brinker, *Coord. Chem. Rev.* 1991, **112**, 81.
17. E. A. Gulliver, T. A. Wark, J. G. Garvey, M. J. Hampden-Smith and A. Datye, *J. Am. Ceram. Soc.* 1991, **74**, 1091.
18. T. A. Wark, E. A. Gulliver, M. J. Hampden-Smith and A. L. Rheingold, *Inorg. Chem.* 1990, **29**, 4360.
19. R. Hani and R. A. Geanangel, *Coord. Chem. Rev.* 1982, **44**, 229.
20. B. A. Vaartstra, J. C. Huffman, P. S. Gradeff, L. G. Hubert-Pfalzgraf, J.-C. Daran, S. Parraud, K. Yunlin and K. G. Caulton, *Inorg. Chem.* 1990, **29**, 3126.
21. D. F. Shriver and M. A. Drezdzon, *The Manipulation of Air-Sensitive Compounds*, 2nd edn, p. 78. Wiley-Interscience, New York (1986).
22. J. Caruso, T. Alam and M. J. Hampden-Smith, *J. Am. Chem. Soc.* 1994, to be submitted.